Proceedings of IMECE'99
1999 ASME International Mechanical Engineering Congress and Exposition
November 14-19, 1999, Nashville, Tennessee, USA

IMECE/DSC-5B-1

INCLUSION PROBING: SIGNAL DETECTION AND HAPTIC PLAYBACK OF 2D FEM AND EXPERIMENTAL DATA

Joseph Yan Paul K. Scott Ronald S. Fearing
Robotics and Intelligent Machines Laboratory
University of California at Berkeley
Berkeley, CA 94720-1774
{joeyan, pkscott, ronf}@robotics.eecs.berkeley.edu

Abstract

The task of probing a medium for an inclusion is cast as a signal detection problem. A sufficient statistic is developed for determining the existence and location of an inclusion. The analysis shows the human limitations of palpation when using a probe and the limitations imposed by a haptic display either when emulating such an environment or when relaying related information in a teleoperated system. Force calculations using FEM models were compared to data measured from constructed gels. Psychophysics experiments demonstrated promising results for the playback of the FEM data.

1 Introduction

Palpation is a procedure frequently employed by physicians to examine tissue using the sense of touch. This technique can be used to distinguish diseased tissue from healthy tissue or to locate hard inclusions, such as tumors, for treatment. Palpation remains important because it is a fast, easy, and cost effective means to perform a diagnosis in many cases.

Understanding the mechanics and psychophysics of palpation can help determine the limits of human ability and the requirements of a haptic display for the task. It is important not only to finding the relationships between various loading parameters (i.e., displacement vs force and/or shape vs pressure distribution) but also how these relationships are perceived by an observer.

In this paper, palpation for inclusions is formulated as a signal detection problem in the presence of noise. All the useful information in an observed vector-valued function is summarized into a single scalar-valued sufficient statistic whose probability distribution under different conditions is known. Comparision of this statistic to a threshold value, which depends on the degree of confidence in the hypothesis, permits the detection of the inclusion. This approach was developed as a simple approximation to how humans may perform this task, but the concepts are amenable to the problem of automated palpation.

Another goal is to compare the playback of simulated and experimental data of palpation on a haptic display to understand the limitations of using such a display in a palpation simulator or a teleoperator. Analysis from the signal detection viewpoint places minimum bounds on the quality of the haptic display.

Several groups have already addressed some basic issues in this area. A short list of some relevant references to general issues in human perception and in haptic interfaces follows: Jones (1998), Fearing *et al* (1997), Salcudean (1997), Srinivasan and LaMotte (1995), Cohn *et al* (1992), Lederman and Browse (1988), and Loomis and Lederman (1986).

Howe *et al* have contributed much work regarding palpation teleoperators, through which a user can remotely make a diagnosis (Howe *et al* (1995), Peine *et al* (1998)). Much of the work describes psychophysics experiments determining specifications required of the sensor and display technologies in order to have effective palpation. Discussion of this application to minimally invasive surgery (MIS) is given by Tendick (1997).

Research in the area of virtual reality palpation training simulators is described by Burdea *et al* (1998) and Langrana *et al* (1997). The simulator consists of the Rutgers Master II force

feedback device and a graphical user interface to provide visual feedback of the user hand location relative to the patient.

Finite element methods (FEM) of palpation to predict tissue response to loads are used by Wellman and Howe (1997) and by Langrana *et al* (1997). Many researchers are using FEMs because they are ideal for addressing the problem of solving partial differential equations for tissues with nonlinear anisotropic properties and complicated geometries.

Tools for automatic palpation are described by Dario and Bergamasco (1988) and Bicchi *et al* (1996). Scilingo *et al* (1997) conducted experiments with a haptic display for simulating surgical tissues. The method described by MacLean (1996) for automatic environment characterization for haptic playback may readily be adapted to quickly estimate complicated tissue mechanical properties.

The remainder of this paper is organized as follows: In section 2, palpation is formulated as a signal detection problem in which a scalar-valued sufficient statistic is derived from the vector-valued response signal. The generation of probe force response data, both calculated from a 2D FEM model and measured using from a force/torque sensor, is described in section 3, followed by results from psychophysics experiments in section 4. The discussion of results and future work is presented in section 5.

2 Probing for inclusions: a signal detection problem

Figure 1 shows an example in which a probe is used for inclusion detection. The probe can be indented into the gel surface and moved laterally while reaction forces are perceived by a user. A rigid probe is used so that a better comparative study can be performed with a haptic display providing only kinesthetic feedback. Although this results in a loss of tactile information, as discussed by Lederman and Klatzky (1999), detection can still be performed because active lateral motion of the probe is permitted to observe changes in compliance under the probe.

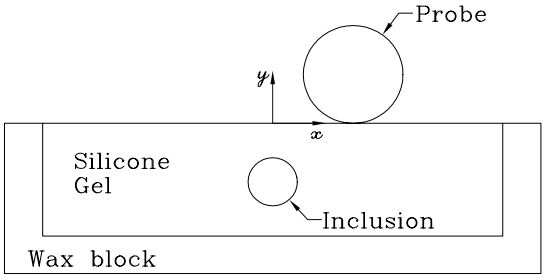

Figure 1. Phantom models

The task of finding the inclusion may be viewed as a signal detection problem, as illustrated in figure 2. In general, the decision as to whether or not a signal is present depends on four factors: (a) prior information available before the stimulus; (b) information about the stimulus; (c) information about the sensor; and (d) the cost of each outcome. A more detailed discussion about general signal detection theory is given by Egan (1975).

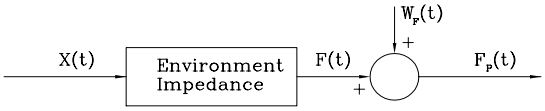

Figure 2. Signal detection problem

Even in our simple model, the ability to detect the inclusion will depend on many parameters. For the inclusion, these include the size, depth, and material properties (larger, more shallow, and stiffer inclusions are more easily detected). For the probe, the size and force/motion range are important (inclusions are easier to detect when the probe is smaller or more deeply indented into the surface). For this detection problem, it is assumed that all these parameters are fixed so that an accurate force response curve can be generated from the commanded trajectory. Given a suitable model for the noise in the perceived force, the task is to determine a sufficient statistic and then establish a threshold for this statistic for varying levels of confidence in being able to detect the inclusion.

In the figure, $\mathbf{X}(t)$ is the probe trajectory, $\mathbf{F}(t)$ is the resulting force on the probe from the environment, and $\mathbf{F_p}(t)$ is the force perceived by the observer. As a crude simplification, $\mathbf{F_p}(t)$ may be viewed as a version of $\mathbf{F}(t)$ corrupted by an additive Gaussian noise signal, $\mathbf{W_F}(t) \sim \mathcal{N}(\mathbf{0}, K_W)$ (i.e., $\mathbf{W_F}(t)$ is zero-mean vector, normally distributed with covariance matrix K_W which gives a measure of the noise spectral power density). $W_F(t)$ can include effects such as sensor noise, surface slip, surface texture, sensor quantization, material or sensor hysteresis, vibration, nonlinearity or other modeling errors. The assumption of a Gaussian distribution allows for easier analysis and for a worst-case scenario. The noise along each of the directions can reasonably be assumed to be independent so $K_W = diag\{\sigma_x^2, \sigma_y^2\}$. For simplicity, we consider the case of a constant depth d and constant velocity v probe trajectory: $\mathbf{X}(t) = [vt \;\; d]^T$

Identify the state that no inclusion exists as $H = 0$ and that an inclusion exists as $H = 1$. To gain a better understanding, first consider the case of determining whether or not an inclusion exists at the lateral position $x = 0$. In this case, for each of the conditions on H, the expected environment force response $\mathbf{F}(t)$ can be readily determined (either from FEM calculations or experimental measurement):

$$\mathbf{F}(t) = \begin{cases} \mathbf{F_0}(t) & \text{if } H = 0 \\ \mathbf{F_1}(t) & \text{if } H = 1 \end{cases} \tag{1}$$

If a decision had to be made based on one component of the vector signal, a matched filter could be used. Consider the

x-component first and define:

$$h_x(t) = \frac{F_{1x}(-t) - F_{0x}(-t)}{\|F_{1x}(-t) - F_{0x}(-t)\|} \tag{2}$$

where the function norm is given by $\|f(t)\| = (\int f^2(t)dt)^{\frac{1}{2}}$ (for convenience, this norm will also be normalized so that the units of $\|f(t)\|$ are the same as those for $f(t)$; this means making t a dimensionless variable). Defining a new signal by the convolution $Y_x(t) = (F_{px}(t) - F_{0x}(t)) * h_x(t)$, then the evaluation of this function at $t = 0$ provides a sufficient statistic to make the decision.

Using (1) yields:

$$Y_x(t) = \begin{cases} W_{Fx}(t) * h_x(t) & \text{if } H = 0 \\ (F_{1x}(t) + W_{F_x}(t)) * h_x(t) & \text{if } H = 1 \end{cases} \tag{3}$$

If $H = 0$, then $Y_x(0) \sim \mathcal{N}(0, \sigma_x^2)$ (this statistic has the same variance as W_{Fx} because $h_x(t)$ is normalized). If $H = 1$, then $Y_x(0) \sim \mathcal{N}(\|F_{1x}(t) - F_{0x}(t)\|, \sigma_x^2)$. Thus, comparing $Y_x(0)$ to some threshold value η_x, one can hypothesize the existence of the inclusion. To include the information content from the y-component, we similarly define the signal:

$$h_y(t) = \frac{F_{1y}(-t) - F_{0y}(-t)}{\|F_{1y}(-t) - F_{0y}(-t)\|} \tag{4}$$

and the vector function:

$$\mathbf{Y}(t) = \begin{bmatrix} h_x(t) & 0 \\ 0 & h_y(t) \end{bmatrix} * (\mathbf{F_p}(t) - \mathbf{F_0}(t)) \tag{5}$$

Then

$$\mathbf{Y}(0) \sim \begin{cases} \mathcal{N}(\mathbf{a}, K_W) & \text{if } H = 0 \\ \mathcal{N}(\mathbf{b}, K_W) & \text{if } H = 1 \end{cases} \tag{6}$$

where, for convenience, the vectors $\mathbf{a} = \begin{bmatrix} 0 \\ 0 \end{bmatrix}$ and $\mathbf{b} = \begin{bmatrix} \|F_{1x}(t) - F_{0x}(t)\| \\ \|F_{1y}(t) - F_{0y}(t)\| \end{bmatrix}$ have been introduced.

The scalar $\gamma = [(\mathbf{b} - \mathbf{a})^T K_W^{-1} (\mathbf{b} - \mathbf{a})]^{1/2}$ is a measure of the signal-to-noise ratio (SNR). Finally, we define the random variable

$$\Theta = (\mathbf{b} - \mathbf{a})^T K_W^{-1} \left(\mathbf{Y}(0) - \frac{\mathbf{b} + \mathbf{a}}{2} \right) \tag{7}$$

Θ is the scalar-valued sufficient statistic that contains all the useful information from the vector-valued function $\mathbf{F_p}(t)$ for the decision to be made. The variance in each of the components of $\mathbf{Y}(0)$ should determine their respective weightings in how reliably they can be used and Θ takes this into account. The probability distribution of Θ, as illustrated in figure 3 for a few values of γ, can be calculated to be:

$$\Theta \sim \begin{cases} \mathcal{N}\left(\frac{-\gamma^2}{2}, \gamma^2\right) & \text{if } H = 0 \\ \mathcal{N}\left(\frac{\gamma^2}{2}, \gamma^2\right) & \text{if } H = 1 \end{cases} \tag{8}$$

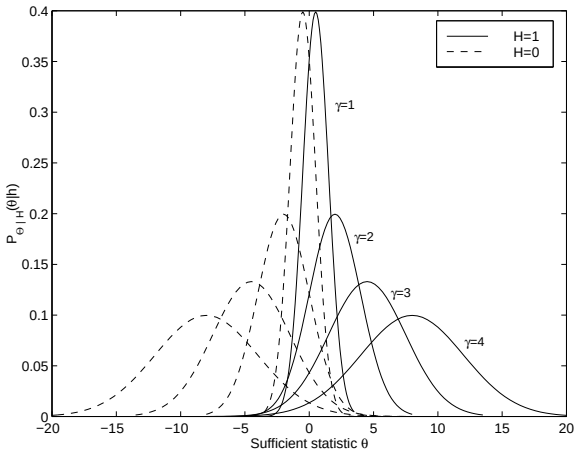

Figure 3. Probability distributions of the sufficient statistic (θ) for several SNR (γ) values

Thus, our method of detection is to evaluate $\mathbf{y}(0)$ from (5), then θ from (7), and based on a threshold value η, make the hypothesis :

$$\hat{H} = \begin{cases} 0 & \text{if } \theta < \eta \\ 1 & \text{if } \theta \geq \eta \end{cases} \tag{9}$$

(Note the subtle distinction between random variables denoted by uppercase letters, and observations denoted by lowercase letters; $\mathbf{Y}(0)$ and Θ are random variables whereas $\mathbf{y}(0)$ and θ are the respective observations of these variables.)

The value of η depends on which criterion is to be used. The maximum a posteriori probability (MAP) rule would maximize the probability of making a correct diagnosis. For the medical procedure of locating tumors, a more appropriate test might be the Neyman-Pearson (NP) criterion in which the false negative rate (the probability of an error given the inclusion exists, denoted by $Pr(e|H = 1)$) is specified and η is chosen to minimize

the false alarm rate ($Pr(e|H=0)$). The dual problem is to maximize the hit rate for a fixed false alarm rate. Figure 4 illustrates how each of these rates can be traded off at the expense of the other for several SNR values. Each curve can be derived by sweeping a vertical line across the graph of figure 3 and specifying point coordinates by the areas to the right of the gaussian for $H=0$ ($Pr(e|H=0)$) and to the left of the gaussian for $H=1$ ($Pr(e|H=1)$).

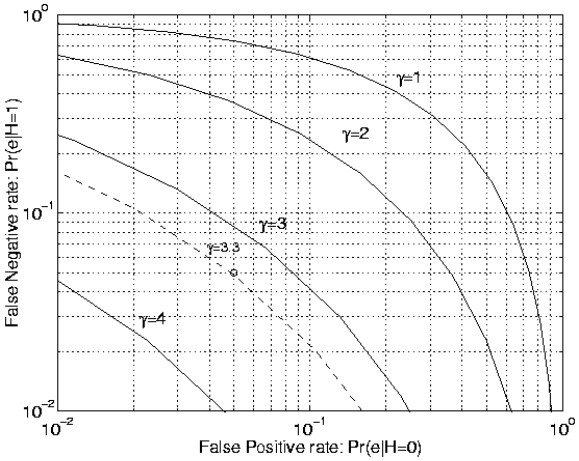

Figure 4. Receiver Operating Characteristic curves demonstrating tradeoffs in error rates for several SNR (γ) values

A concrete example of determining a haptic display requirement using figure 4 would be to specify a minimum 95% hit rate ($Pr(e|H=1) \leq 0.05$) and maximum 5% false alarm rate ($Pr(e|H=0) \leq 0.05$). This point is marked on the graph and requires $\gamma > 3.3$. If the force signal difference is roughly $0.5N$, then the overall noise level needs to be less than $0.5N/\gamma = 0.15N$. Using a nominal absolute force level of $1.6N$, the human operating noise level is estimated at $0.1N$ (see Jones (1998)) so the haptic display must introduce less than $(.15^2 - 0.1^2)^{1/2}N = 0.11N$ of noise to maintain the required SNR, assuming the noise sources are independent and their variances add. The haptic display error variance due to quantization alone is given by $\sigma_e^2 = \frac{\Delta^2}{12}$, where Δ is the force resolution.

The results can be generalized to colored noise, for which the covariance matrix is known, by using the standard method of applying a whitening filter and reducing the problem to the one which has already been solved.

The problem can also readily be modified to estimate the detected inclusion location. If the inclusion lateral position is $x = x_{incl}$, then $\mathbf{Y}(v/x_{incl})$ would have the distribution specified in (6). Without any noise, each component of $\mathbf{Y}(t)$ would be maximized at $t = v/x_{incl}$. Thus, (7) would be left as a function of t:

$$\Theta(t) = (\mathbf{b}-\mathbf{a})^T K_W^{-1} \left(\mathbf{Y}(t) - \frac{\mathbf{b}+\mathbf{a}}{2} \right) \tag{10}$$

Θ_{max} would be the new sufficient statistic to answer the detection problem and the value t_{incl} such that $\Theta(t_{incl}) = \Theta_{max}$ gives the estimated inclusion position as $x_{incl} = vt_{incl}$. The statistics for Θ_{max} are not the same as in (8) and they become much more complicated but the overall result is that the test will be more conservative in the sense that $Pr(e|H=1)$ will not increase (*i.e.* there is an even lower chance that an inclusion will be missed).

3 Data Collection

Five phantom gel models were created for the signal detection problem. Each model was constructed from a wax block with a 15.0*mm* deep well, 34.0*mm* wide and 59.2*mm* long, filled with a silicone gel (GE RTV6166). A 0.5*mm* thick layer of rubber (Dow Corning HS3) was added to protect the gel and provide a surface which can easily be lubricated. In four models, a 30*mm* long, 6.4*mm* diameter latex tube was embedded in the gel at depths of 2.6*mm* to 8.6*mm* (in increments of 2mm) from the surface. The fifth model had no inclusion and acted as a reference. A lubricant (AHP, Inc. PAM vegetable oil spray) was applied to the surface to reduce the effects of friction. In all the experiments, the rigid probe is semicylindrical, 30*mm* long, and 13*mm* in diameter. The reason for using cylindrical probes and inclusions is that it permits a more appropriate comparison to the 2D FEM models.

3.1 Finite Element Method Data

Calculations using FEM models were used to predict all the reaction forces under the various loads. A 2D FEM model of the constructed gels was generated using the commercial software package, Marc/Mentat. In the current model, dynamic effects have been ignored and the interface between the probe and the gel surface is frictionless. Further simplifying conditions are that all the materials are linear, isotropic, and nearly incompressible with a Poisson ratio of 0.49. The Young's moduli were roughly determined to be $E_{gel} = 5000N/m^2$, $E_{HS3} = 1.8 \times 10^5 N/m^2$ and $E_{incl} = 1.2 \times 10^6 N/m^2$). Fixed displacement boundary conditions were placed on the the gel where it meets the wax block.

As the probe is moved to depths up to 4mm and lateral positions up to 10mm relative to the origin, the forces per unit length exerted on it were calculated and recorded. The force curves in figure 5 were generated for the model with an inclusion 2.6*mm* deep. Calculations were only performed for positive lateral positions and symmetry was used to determine the forces for negative lateral positions. The qualitative features of the graphs are consistent with intuition.

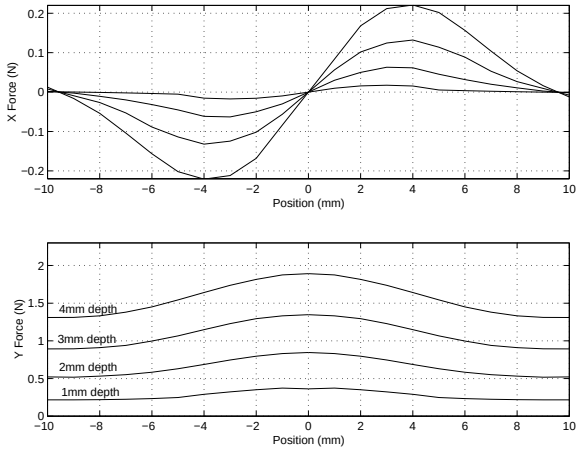

Figure 5. FEM Force curves for model with inclusion $2.6mm$ deep

Figure 6 graphically shows how the model deforms under a load from the probe. The mesh of the shaded circular inclusion is visible and barely deforms because it is significantly more stiff than the surrounding material.

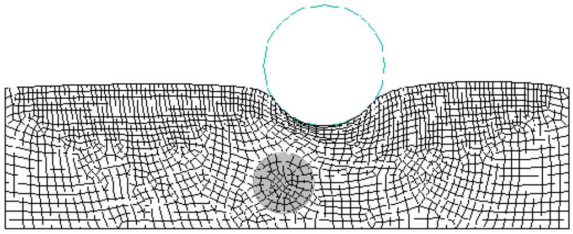

Figure 6. Deformation using FEM

3.2 Measured data

Data was collected with the setup in figure 8. Two linear positioning stages allow accurate positioning of a 6 DOF ATI Nano-force/torque sensor on which the semicylindrical probe is mounted. Probe forces were measured at $1mm$ intervals in both indentation depth and lateral position. The resulting lateral and normal force components as a function of displacement for the gel with the $2.6mm$ deep inclusion are shown in figure 7, which should be compared to figure 5. The qualitative features are similar while the quantitative values are reasonably close, considering that a simple model with very roughly determined material properties was used in the FEM calculations.

4 Psychophysics Experiments

Psychophysics experiments were performed on 10 human subjects. There were 6 males and 4 females ranging in age from 20 to 30 years (mean 24.5 years). Two subjects were familiar with the experimental procedure and apparatus.

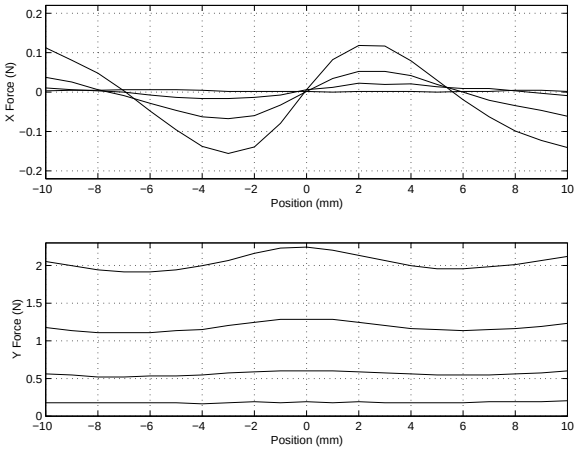

Figure 7. Experimental Force curves for gel with inclusion $2.6mm$ deep

The design of the experiments is summarized in figure 8. In one experiment, the subject can interact directly with the gel using a probe attached at the index finger. Another test involves the playback of the force data calculated using FEM models on a haptic display. The last experiment uses the measured force data from an instrumented probe instead of the FEM data.

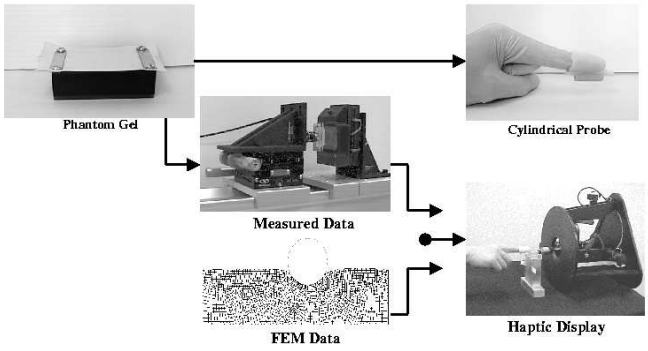

Figure 8. Overview of psychophysics experiments

In all of the experiments, forced-choice testing was performed in which a pair of samples (of which, only one would contain an inclusion) was presented to the subject, each for only 3 seconds. The subject had to guess which sample had the inclusion. 30 trials for each of the four inclusion depths were tested under all three experiments (360 pair-wise tests per subject, in total). The probability of correctly guessing from the pair can be calculated as a function of γ using knowledge of the probability functions in (8) and this relation is displayed in figure 9.

An Immersion Laparoscopic Impulse Engine controlled by a PC operating under Linux was used for playback of data. The force data for playback is stored in two matrices (one for the lateral forces and the other for normal forces) with the rows and

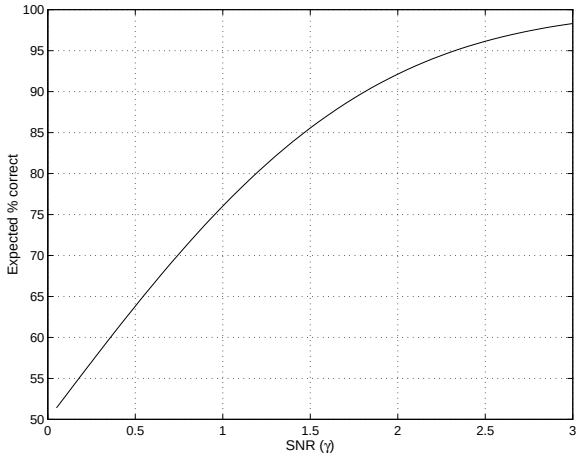

Figure 9. Probability of choosing correctly in pair-wise tests

columns associated with the depths and lateral positions, respectively. Simple linear interpolation of the forces is used when the operation is within the bounds of the data and linear extrapolation is used outside these bounds.

Measurements of the forces applied by the haptic display indicate that the standard deviation in the error of the force is roughly $0.024N$ and this may become a dominant noise term for the tangential force component. This noise is primarily due to backlash and friction while quantization introduces only $0.5mN$ of noise.

4.1 Direct Contact with Gels

In this experiment, subjects have a plastic mold placed on the index finger to remove spatial contact information (Lederman (1999)). The mold has a semicylindrical probe at the bottom, with the same dimensions as the probe used in the collection of measurement data. A brief training period was permitted in which the subject probed each gel specimen. Mechanical limits prevented the probe from being indented more than $4mm$. A cloth screen was used to hide visual cues. The raw data from these tests are tabulated in Table 1 and graphically represented in figure 10.

4.2 Haptic Display Data Playback

Using the haptic display to interact with the virtual gels, subjects performed the same pair-wise testing using FEM and measured data. A mechanical stop limited the amount of indentation to $4mm$. Furthermore, sandpaper at the mechanical stop was used to deter the subject from sliding the probe along this limit. A brief training program was used to acquaint the subjects with the test. The results are summarized in Table 1 and figures 11 and 12.

Figure 13 compares all three experiments. The error bars give 95% confidence intervals for proportion (see Natrella (1963)). The results from the direct contact and the playback of FEM data are quite close.

Table 1: Number of correct responses in 30 trials

Incl depth (mm)	2.6	4.6	6.6	8.6
sbjct 1/direct contact	30	28	27	27
sbjct 2/direct contact	30	30	28	23
sbjct 3/direct contact	30	29	20	21
sbjct 4/direct contact	28	25	18	16
sbjct 5/direct contact	27	26	23	19
sbjct 6/direct contact	30	30	27	17
sbjct 7/direct contact	23	19	18	13
sbjct 8/direct contact	30	30	30	19
sbjct 9/direct contact	30	30	29	23
sbjct 10/direct contact	30	28	27	22
Direct contact mean	28.8	27.5	24.7	20.0
sbjct 1/FEM data	30	30	30	21
sbjct 2/FEM data	30	30	29	25
sbjct 3/FEM data	30	29	28	16
sbjct 4/FEM data	28	29	24	20
sbjct 5/FEM data	29	25	20	17
sbjct 6/FEM data	29	29	27	15
sbjct 7/FEM data	27	23	18	15
sbjct 8/FEM data	30	30	27	20
sbjct 9/FEM data	29	24	21	16
sbjct 10/FEM data	30	28	29	24
FEM data mean	29.2	27.7	25.3	18.9
sbjct 1/measured data	30	22	24	18
sbjct 2/measured data	30	28	28	21
sbjct 3/measured data	28	27	19	15
sbjct 4/measured data	25	19	19	21
sbjct 5/measured data	29	24	23	18
sbjct 6/measured data	26	21	23	17
sbjct 7/measured data	17	15	19	18
sbjct 8/measured data	29	26	26	13
sbjct 9/measured data	26	21	22	15
sbjct 10/measured data	28	25	26	18
Measured data mean	26.8	22.8	22.9	17.4

5 Discussion and Future Work

Palpation has been framed as a signal detection problem and a sufficient statistic has been developed. Use of the NP criterion can establish the threshold on the statistic to minimize the false positive rate under a specified maximum false negative rate. An example was presented in which specified maximum error probabilities determined the required SNR, which in turn bounded the noise tolerated in the haptic display. Alternatively, the specified SNR can determine the necessary indentation force to achieve a sufficiently strong signal. These problems were solved for a set of fixed parameters but a more general approach would use probability distributions of these parameters (for example, when the inclusions to be detected occur at different depths with differing probabilities). It is not difficult to see how the problem may be further modified to address other questions such as the maximum inclusion depth or minimum inclusion size which can be accurately detected.

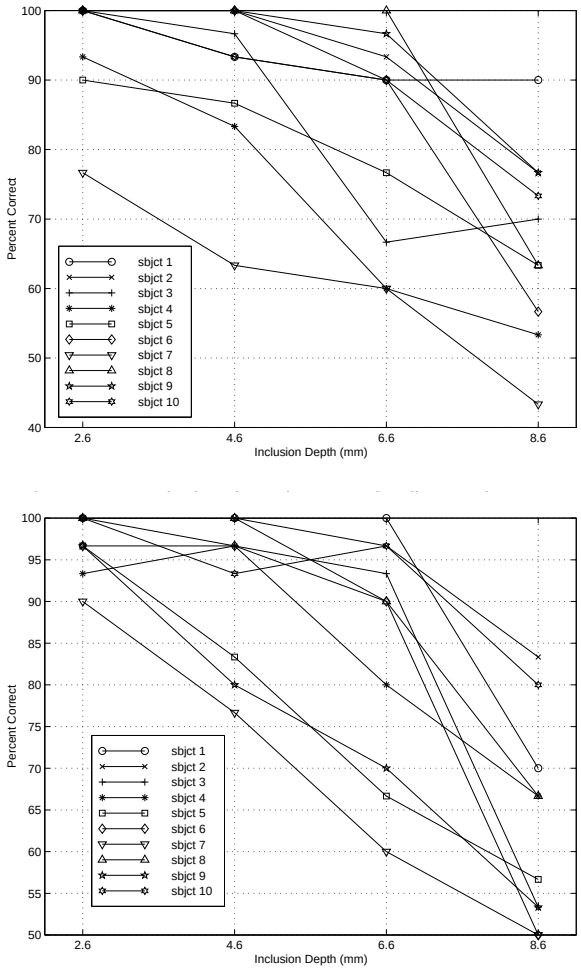

Figure 11. Inclusion detection rates for FEM data playback

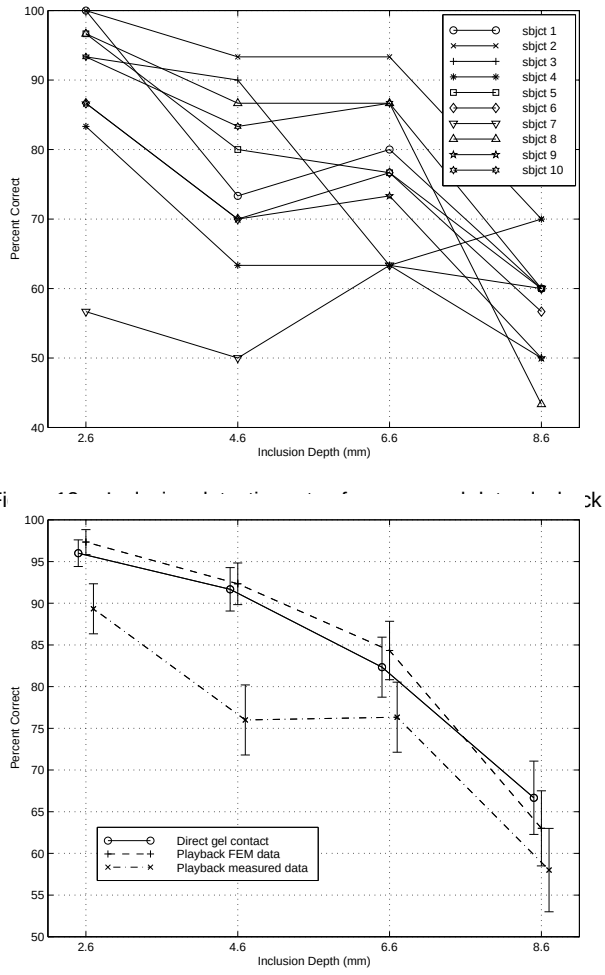

Figure 13. Comparison of correct inclusion detection rates, using 95% confidence intervals for proportion

The psychophysics experiments demonstrated similar results between the playback of FEM data and the direct contact with the true gels, with very close inclusion detection rates. However, the results using the the played back measured data do not compare as well. From figures 5 and 7, the differences may be explained from the relative size of the tangential forces and/or the slopes of the normal forces. Discrepancies with the direct contact experiment may arise from several sources such as friction (which appears to be significant in experiments but was ignored in the FEM) and vision (the user could see the level of indentation with the haptic display but not the true gels).

A rough analysis of the noise contributions can be performed using the noise estimates summarized in Table 2. Considering the case of the $6.6mm$ deep inclusion, playback of FEM data gave a 84% accuracy which, interpolating from figure 9, indicates that the subjects are operating near $\gamma = 1.45$. The peak signal strength for this inclusion is $340mN$ so the noise estimate from the psychophysics experiments is $235mN$. The noise estimate for the FEM playback using the applicable noise sources from Table 2 is $170mN$ (dominated by the actuation backdrive friction), which is reasonable given the confidence intervals. The noise estimate for the direct contact case using the appropriate noise sources is $220mN$ (dominated by unmodelled contact forces).

Table 2: Noise estimates

Source	Noise level
Sensor (ATI)	$20mN$
Actuation quantization (Immersion)	$0.5mN$
Actuation backdrive friction (Immersion)	$140mN$
Unmodelled direct contact (friction, hysteresis, nonlinearity, etc)	$200mN$
Human perception (Jones (1998))	$93mN$

Palpation using direct contact of the fingerpad to the surface allows the mechanoreceptors to provide pressure distribution information and this makes the detection task much easier than when using a rigid probe as described in the paper. The

rigid probe was used here so a better comparative study could be conducted in our experiments. Modification of the approach to include complete tactile information rather than simply forces will be done and this may be used to determine the specifications of a tactile display.

The calculations using the FEM models compare well to the measurements although very simple models were used. Future work here includes the use of nonlinear anisotropic material models with complicated 3D geometries undergoing large deformations to provide more realistic tissue behavior. Studies should be performed to determine how well humans can distinguish parameters such as inclusion depth, location, stiffness and size.

The model will become more complicated as our understanding of the task grows. For example, a multiplicative noise model may be more appropriate than an additive one in order to account for Weber's law in which the mechanoreceptor noise level grows with the force level. Table 2 provides a preliminary look at various noise contributions but a more detailed exploration of the nature and significance of each source will be performed. Also, an impedance model for the user in which the commanded trajectory is tracked rather than followed may be more realistic.

Although the method was developed to understand human palpation abilities, the signal detection approach may also prove useful in automatic inclusion detection or augmented detection to give an objective measure to the physician on the likelihood of a tumor.

6 Acknowledgements

The authors thank K. Chiang, G. Moy, J. Hsu, A. Sherman and N. Dhruv for useful comments and discussions. Thanks also to the volunteer participants in the experiments. Support of this work by NSF grant IRI-9531837 is gratefully acknowledged.

REFERENCES

A. Bicchi, G. Canepa, D. De Rossi, P. Iacconi, and E.P. Scilingo. A sensorized minimally invasive surgery tool for detecting tissutal elastic properties. In *Proc of the IEEE Intl Conf on Robotics and Automation*, pages 884–888, Minneapolis, USA, April 1996.

G.C. Burdea, G. Patounakis, V. Popescu, and R.E. Weiss. Virtual reality training for the diagnosis of prostate cancer. In *IEEE Symp on Virtual Reality and Applications*, pages 190–197, Atlanta, Georgia, Mar 1998.

M.B. Cohn, M. Lam, and R.S. Fearing. Tactile feedback for teleoperation. In *Proc of the SPIE - The Intl Society for Optical Eng*, volume 1833, pages 240–254, Boston, MA, Nov 1992.

P. Dario and M. Bergamasco. An advanced robot system for automated diagnostic tasks through palpation. *IEEE Trans on Biomedical Eng*, 35(2):118–126, Feb 1988.

J.P. Egan. *Signal detection theory and ROC Analysis*. Academic Press, Inc., 1975.

R.S. Fearing, G. Moy, and E. Tan. Some basic issues in teletaction. In *Proc of the IEEE Intl Conf on Robotics and Automation*, Albuquerque, NM, April 1997.

R.D. Howe, W.J. Peine, D.A. Kontarinis, and J.S. Son. Remote palpation technology. *IEEE Eng in Med and Biol Magazine*, pages 318–323, May/June 1995.

L.A. Jones, Perception and control of finger forces. *Proc of the ASME Dyn Sys and Control Div*, volume 64, pages 133–137, Anaheim, CA, Nov 1998.

N.A. Langrana, G. Burdea, J. Ladeji, and M. Dinsmore. Human performance using virtual reality tumor palpation simulation. *Computers & Graphics*, pages 451–458, Apr 1997.

S.J. Lederman and R.A. Browse. *The Physiology and Psychophysics of Touch*, pages 71–91. Springer-Verlag, Berlin, 1988.

S.J. Lederman and R.A. Klatzky. Sensing and displaying spatially distributed fingertip forces in haptic interfaces for teleoperator and virtual environment systems. In *Presence*, vol 8, no 1, pages 86–103, Feb 1999.

J.M. Loomis and S.J. Lederman. Tactual perception. In K.R. Boff, L. Kaufman, and J.P. Thomas, editors, *Handbook of Perception and Human Performance*, pages 31–41. John Wiley and Sons, New York, 1986.

K.E. MacLean. The "haptic camera": A technique for characterizing and playing back haptic properties of real environments. In *Proc of the ASME Dyn Sys and Control Div*, pages 459–467, 1996.

M.G. Natrella. Tables. In *Experimental Statistics, Handbook 91*, page T-47. National Bureau of Standards, Washington, DC, 1963.

W.J. Peine and R.D. Howe. Do humans sense finger deformation or distributed pressure to detect lumps in soft tissue? In *Proc of the ASME Dyn Sys and Control Div*, volume 64, pages 273–278, Anaheim, California, Nov 1998.

S.E. Salcudean. Control for teleoperation and haptic interfaces. In B. Siciliano and K.P. Valavanis, editors, *Control Problems in Robotics and Automation*, pages 50–66. Springer Verlag, 1997.

E.P. Scilingo, D. De Rossi, and A. Bicchi. Haptic display for replication of rheological behaviour of surgical tissues: modelling, control and experiments. In *Proc of the ASME Dyn Sys and Control Div*, pages 173–176, 1997.

M.A. Srinivasan and R.H. LaMotte. Tactual discrimination of softness. In *Journal of Neurophysiology*, pages 88–101, Jan 1995.

F. Tendick and M.C. Cavusoglu. Human machine interfaces for minimally invasive surgery. In *Proc of the 19th Annual Intl Conf of the IEEE Eng in Medicine and Biology Society*, Chicago, IL, Nov 1997.

P.S. Wellman and R.D. Howe. Modeling probe and tissue interaction for tumor feature extraction. In *ASME Summer Bioeng*

Conf 1997, Sun River, Oregon, June 1997.